

A Deep Learning Model of Histologic Tumor Differentiation as a Prognostic Tool in Hepatocellular Carcinoma

Anastasiia Deviataieva

Introduction

- **Hepatocellular carcinoma (HCC)**, the most common primary liver cancer and the third most common cause of cancer- related death worldwide.
- “tumor differentiation” refers to the extent to which cancers histologically resemble or recapitulate their normal tissue counterpart.
- Histologic features of tumor differentiation in HCC include cytoarchitecture, immunohistochemistry profile, and reticulin framework.
- Traditional approach: Edmondson-Steiner and World Health Organization (WHO) grading systems.
- **AI approach:** a supervised deep-learning model to quantify differentiation features digitally, aiming to improve prognostic predictions.

| Reference | Grades | Architecture | Cytology | Other features |
|--------------------------------|---------------------------|--|--|--|
| World Health Organization (21) | Well differentiated | Thin trabecular, frequent acinar structures | Minimal atypia | Fatty change is frequent |
| | Moderately differentiated | Trabecular (3 or more cells in thickness) and acinar | Abundant eosinophilic cytoplasm, round nuclei with distinct nucleoli | Bile or proteinaceous fluid within acini |
| | Poorly differentiated | Solid | Moderate to marked pleomorphism | Absence of sinusoid-like blood spaces |
| | Undifferentiated | Solid | Little cytoplasm, spindle, or round-shaped cells | — |
| Edmondson and Steiner (13) | Grade I | — | — | Areas of carcinoma where distinction from hyperplastic liver is difficult |
| | Grade II | Trabecular, frequent acini (lumen varying from tiny canaliculi to large thyroid-like spaces) | Resemblance to normal hepatic cells; larger nuclei; abundant acidophilic cytoplasm | Cell borders sharp and clear cut; acini containing bile or protein precipitate |
| | Grade III | Distortion of trabecular structure, acini less frequent than grade II | Larger, more hyperchromatic nuclei, granular but less acidophilic cytoplasm | Acini are less frequent; tumor giant cells may be numerous |
| | Grade IV | Medullary, less trabeculae, rare acini | Highly hyperchromatic nuclei, scanty cytoplasm, with fewer granules | Loss of cell cohesiveness; giant, spindle or short-plump cells can be found |

Figure 1. Histological features from Edmondson and Steiner (ES) publication and WHO book. (Martins-Filho et al., 2017)

Materials

Cohort: 99 HCC patients with curative resection (retrospective)

Data: Digitized histopathology slides for each tumor:

- H&E (Hematoxylin & Eosin) for morphology
- Reticulin stain: Reveals the network of supporting fibers; loss of reticulin → poorly differentiated HCC
- IHC for HepPar-1 (marker of hepatocytic differentiation; high expression in well-differentiated cell) and Glypican-3 (oncofetal antigen) tumor differentiation markers

Outcomes Measured: Overall survival, disease-free survival, time to metastasis, local recurrence

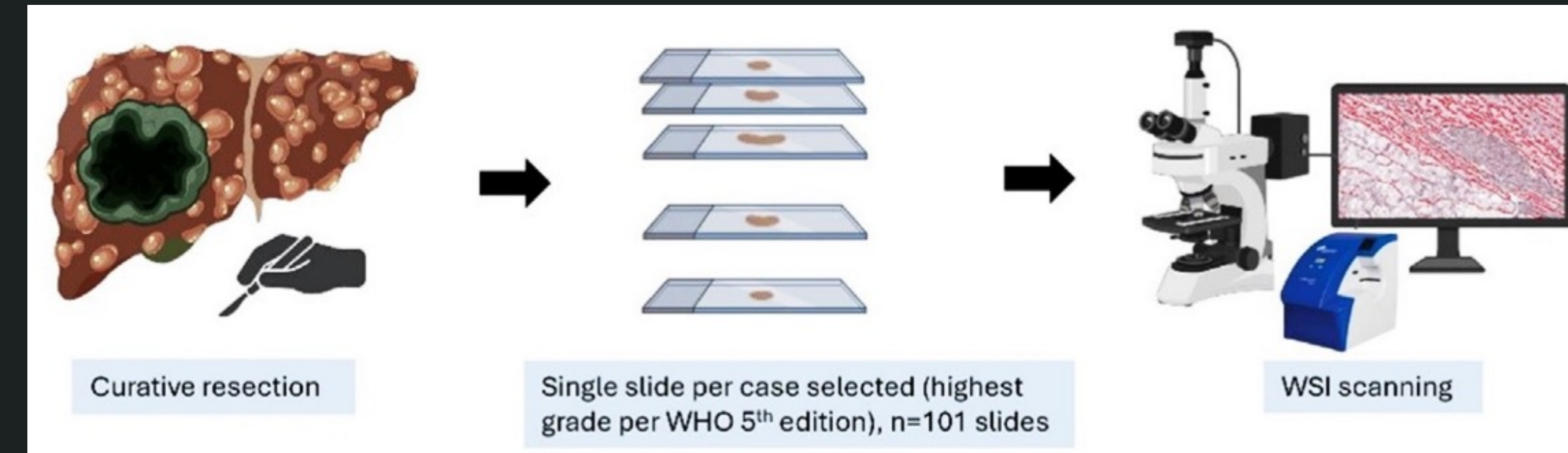


Figure 2. Image extracting workflow. After curative liver resection, one highest-grade slide from each case (n = 101) is selected and digitized through whole-slide imaging for subsequent computational analysis. (Patil et al., 2025). Liver tissue samples were fixed in 10% neutral buffered formalin, embedded in paraffin, cut at 4-mm sections, and stained with H&E, HepPar 1, glypican-3 (GPC) immunostains, and reticulin protocols.

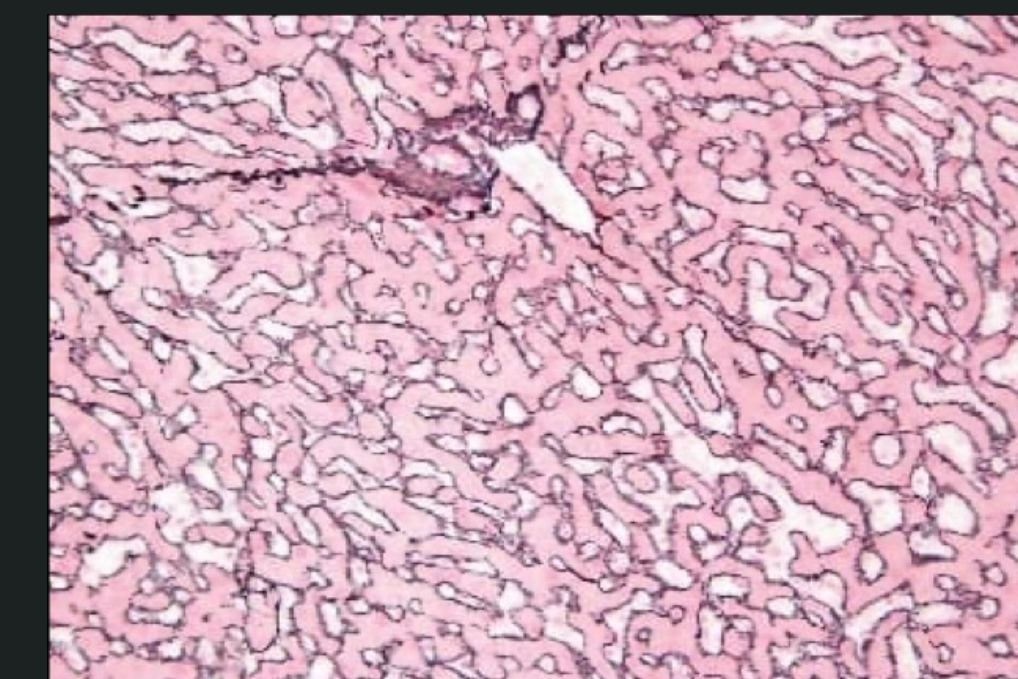


Figure 3. Reticulum II Staining Kit on liver tissue. Reticulum II Staining Kit stains reticulin fibers black against a red pink (Nuclear Fast Red counterstain) background. (ScyTek Laboratories, n.d.)

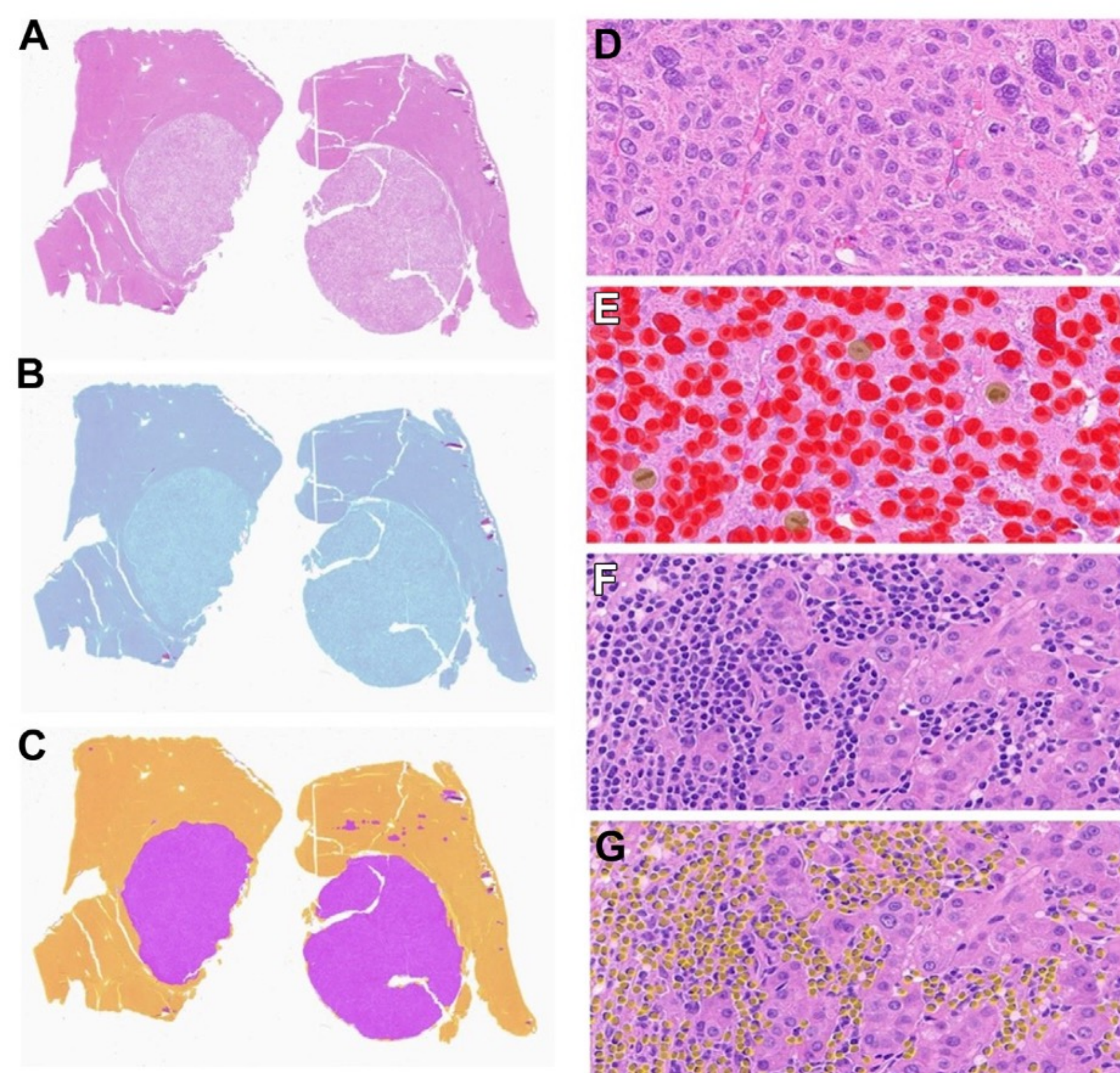


Figure 4. AI model for automated recognition of histologic features of HCC. (A) Hematoxylin and eosin stain, (B) general tissue detector algorithm with automated artifact exclusion (light blue), and (C) automated tumor (purple) and nonneoplastic liver tissue (yellow) detection. (D) HCC hematoxylin and eosin stain (E) with object recognition of hepatocyte nuclei (red) and mitotic figures (brown) and (F) intratumoral lymphocytes (G) with automated tumor-infiltrating lymphocyte detection. (H) HCC reticulin stain and (I) automated quantitative analysis of reticulin fibers. HCC immunostains with automated quantitative analysis of (J) glypican-3 and (K) HepPar 1. HCC, hepatocellular carcinoma. (Patil et al., 2025)

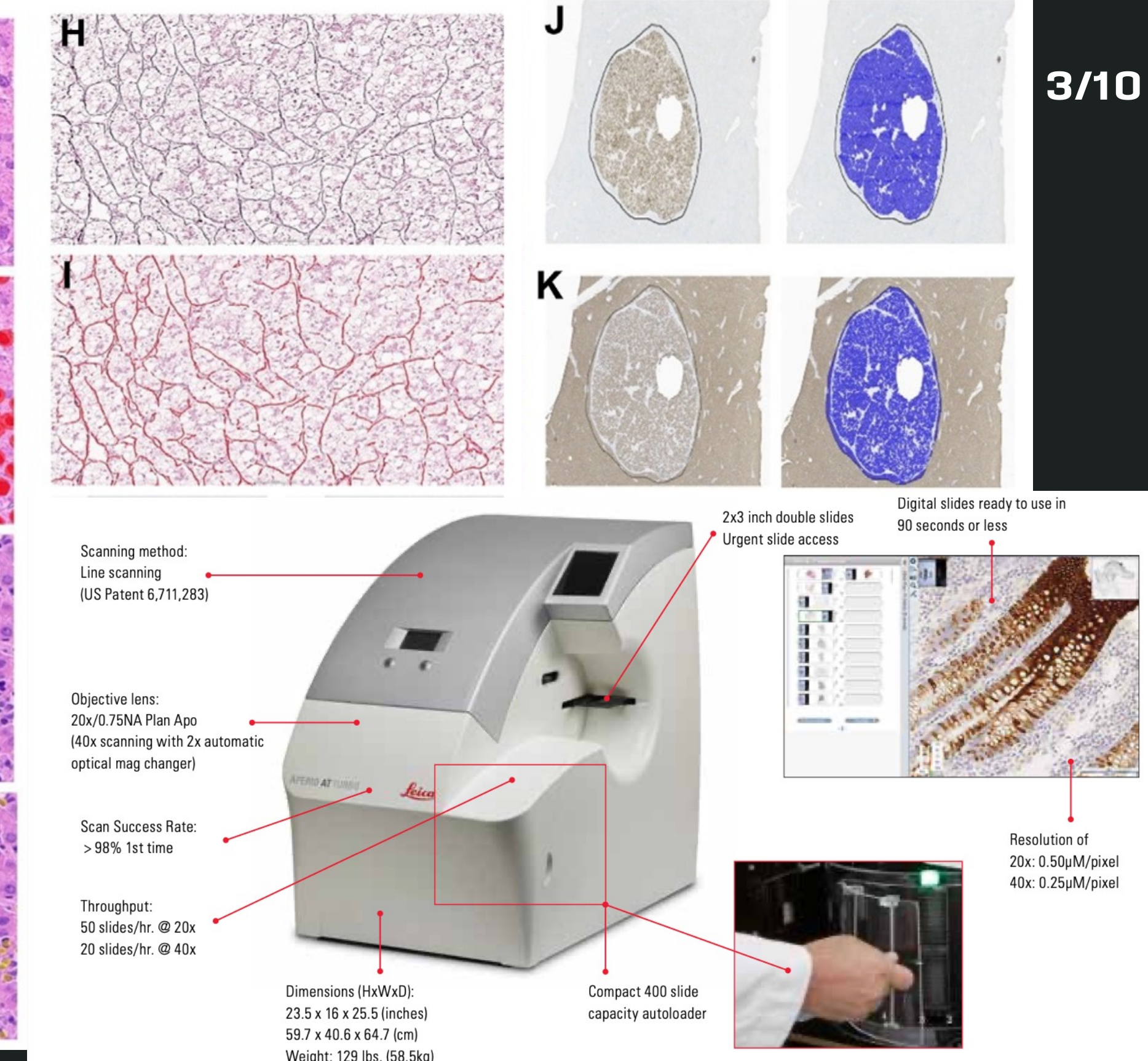


Figure 5. Aperio ScanScope AT Turbo, a bright-field scanning instrument by Leica Biosystem (ScyTek Laboratories, n.d.).

AI Model Workflow

Platform: Used a cloud-based convolutional neural network platform (Aiforia Technologies) for supervised learning.

Tumor segmentation: model distinguished tumor tissue from benign (tissue detector, artifact removal).

Feature detection

- Nuclear morphology: density (cellularity), nuclear area, shape circularity, chromatin texture, cell pleomorphism
 - Mitoses: automated detection of mitotic figures (cell divisions)
 - IHC: percentage of tumor cells positive for HepPar-1 and for Glypican-3
 - Reticulin framework: proportion of area with reticulin fibers (comparison to normal liver)

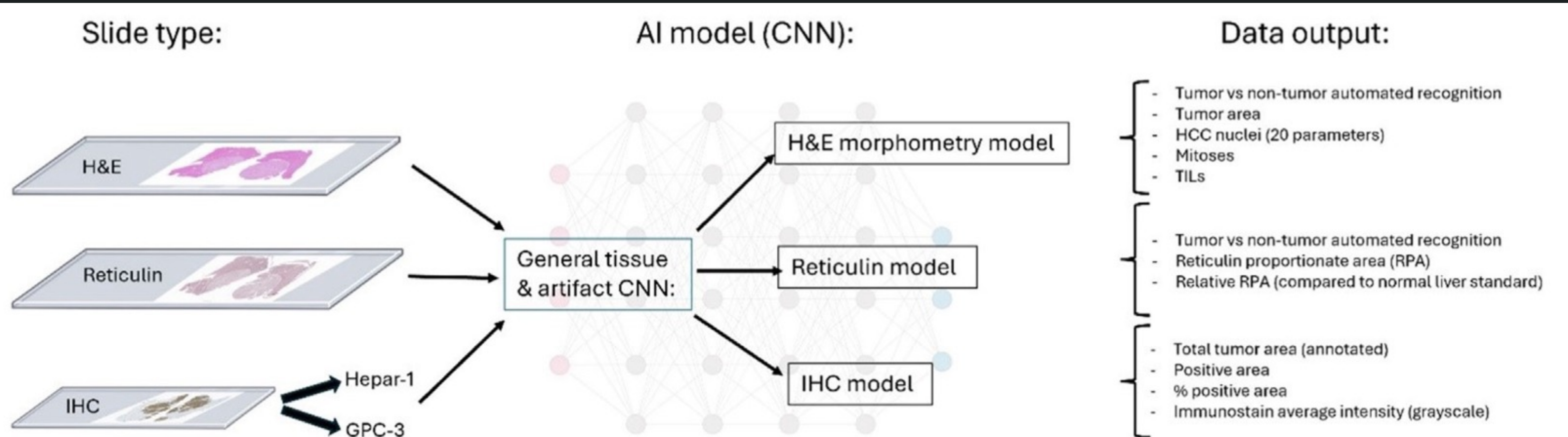


Figure 6. AI model development (Patil et al., 2025)

CNNs Architecture

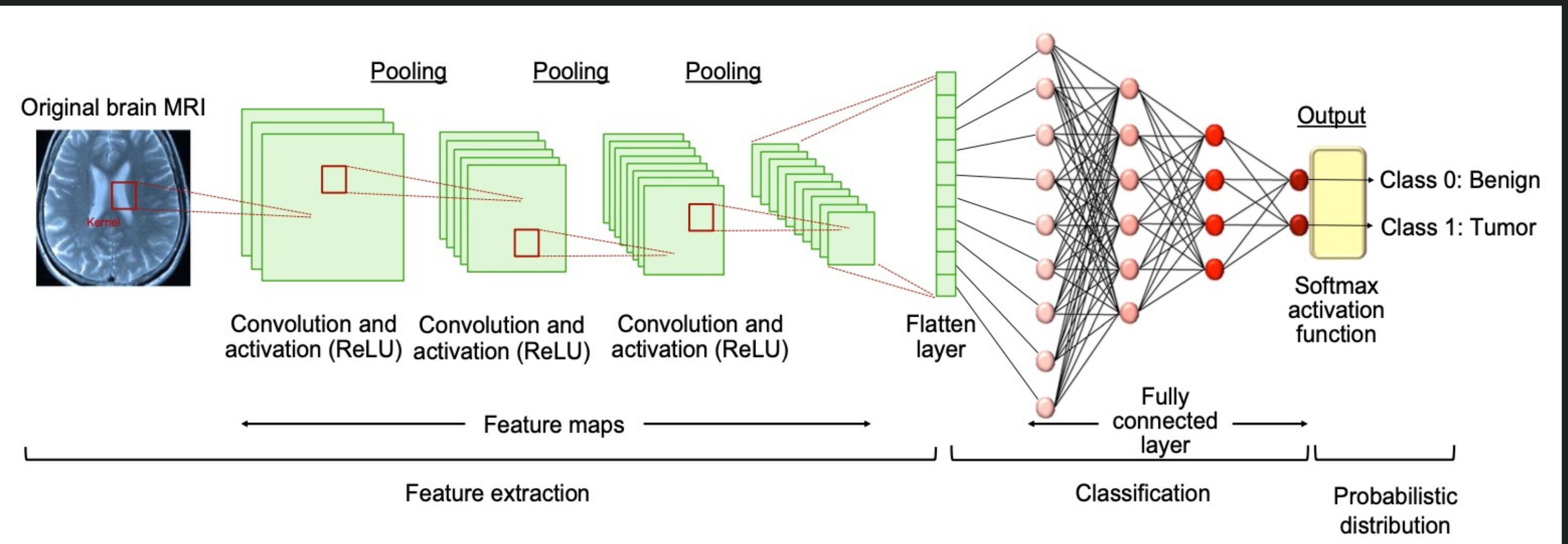


Figure 7. An example of medical image analysis using CNN architecture (brain MRI). (Takahashi et al., 2024)

CNN Pipeline – Generic Form:

- Input – raw image or multi-channel data array
- Convolution + Activation (e.g., ReLU) – sliding kernels generate local feature maps
- Pooling / Sub-sampling – shrink spatial size while retaining salient responses
- Stacked Convolutional Blocks – wider receptive fields, progressively abstract features
- Flatten or Global Pooling – convert 3-D feature tensor to 1-D feature vector
- Fully Connected layer(s) – integrate all learned features
- Output head (Softmax, Sigmoid, etc.) – produces final class probabilities or regression values

Statistical Analysis

Modeling: Built Cox proportional-hazards models for outcomes (overall survival, disease-free survival, metastasis, recurrence).

Comparisons: Tested models using routine data vs. models including AI-derived features.

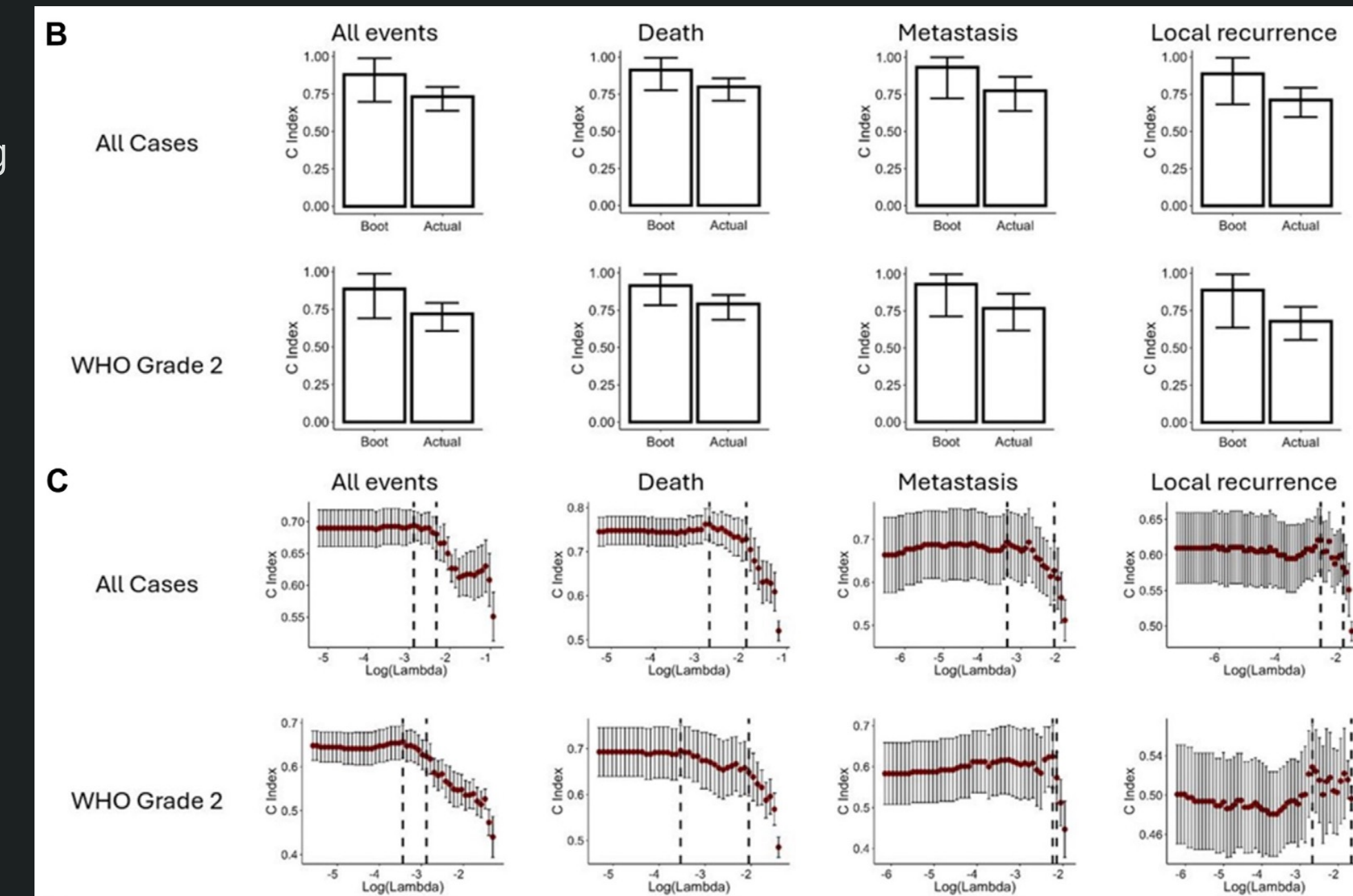
Metrics: Evaluated using concordance index (C-index) - higher is better predictive accuracy.

Validation: Performed bootstrap resampling to estimate confidence intervals

Feature selection: Applied LASSO regression to select the most informative features and avoid overfitting

| Statistical model | Variables included |
|-------------------|---|
| Base Path | <ul style="list-style-type: none"> WHO grade AJCC pT stage |
| AI Path | <ul style="list-style-type: none"> Up to 5 selected AI-quantified features |
| Full Path | <ul style="list-style-type: none"> WHO grade AJCC pT stage Up to 5 selected AI-quantified features |
| Base ClinPath | <ul style="list-style-type: none"> WHO grade AJCC pT stage Age Sex |
| Full ClinPath | <ul style="list-style-type: none"> WHO grade AJCC pT stage Age (y) Sex Up to 5 selected AI-quantified features |

Figure 8. Clinical and pathologic variables included in each statistical model. (Patil et al., 2025)



Results

Statistical models that included these AI-based variables outperformed models with combined clinical pathologic features:

- overall survival (C-indexes of 0.81 vs 0.68),
- disease-free survival (C-indexes of 0.73 vs 0.68),
- metastasis (C-indexes of 0.78 vs 0.65),
- local recurrence (C-indexes of 0.72 vs 0.68)

for all cases, with similar results in the subgroup analysis of WHO grade 2 HCCs.

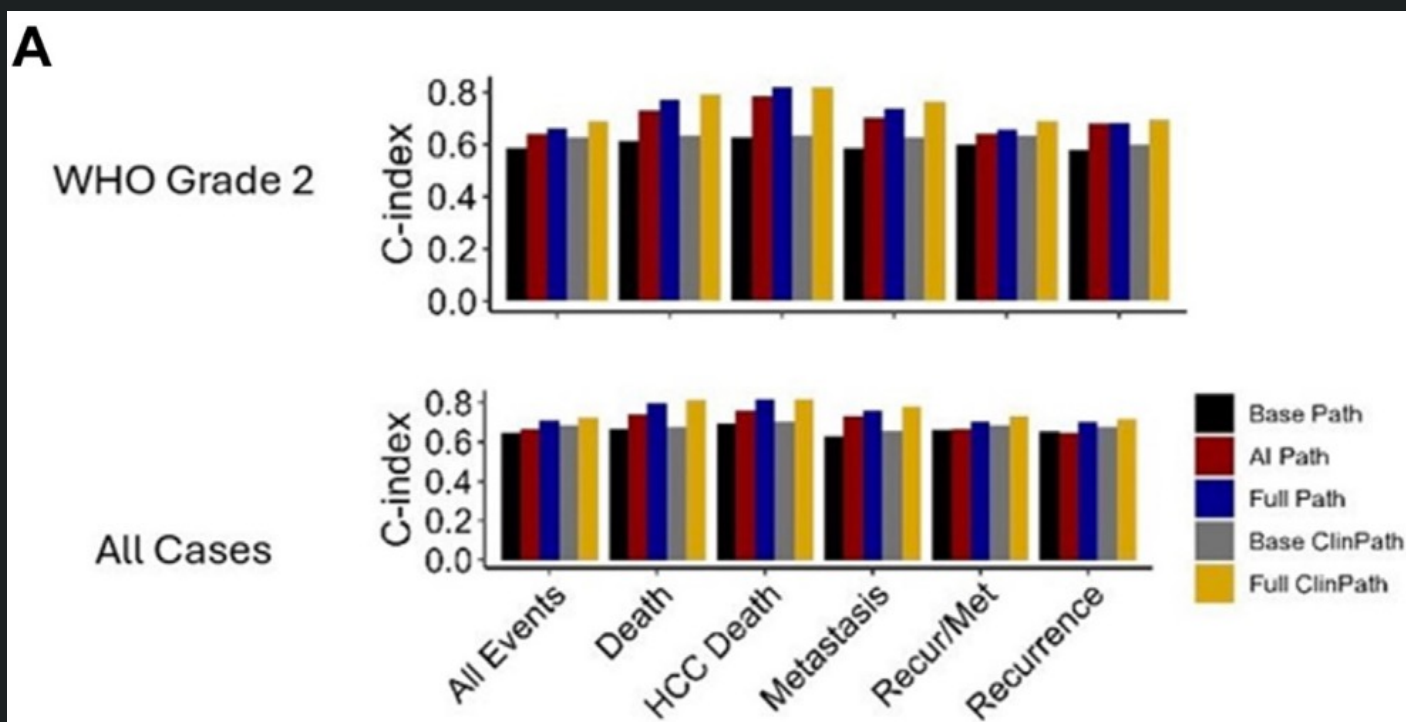


Figure 10. C-index for statistical models, including different combinations of clinical (routine), pathologic, and AI modele generated data. (Patil et al., 2025)

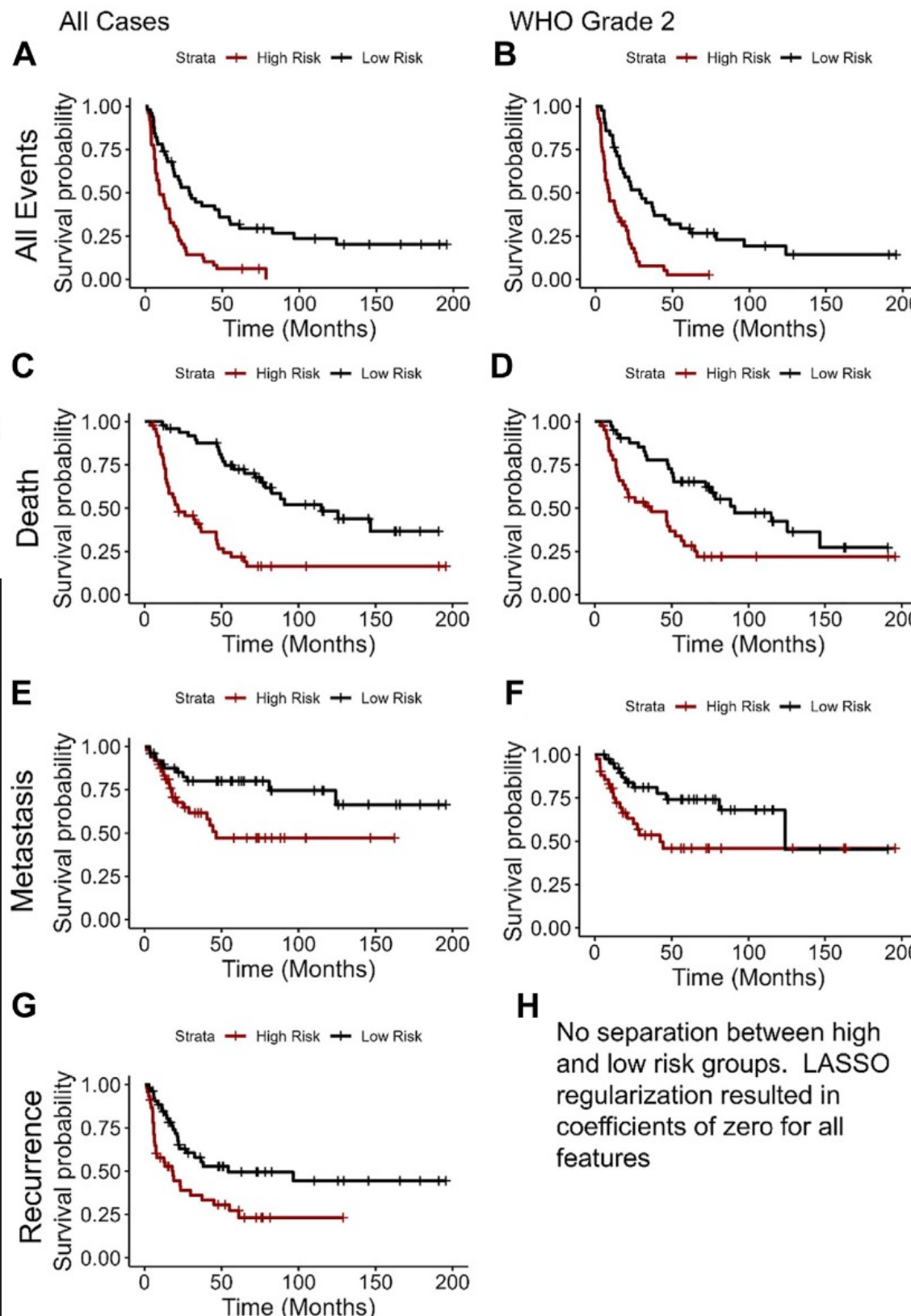


Figure 11. Kaplan-Meier survival curves for high-risk and low-risk groups across clinical outcomes. Survival probabilities over time for patients stratified into high-risk and low-risk groups based on model predictions for both all cases and WHO grade 2 cases specifically..(Patil et al., 2025)

| Variable | Description |
|--|--|
| 1. pT stage | "T" component of the <i>AJCC Cancer Staging Manual</i> , eighth edition |
| 2. World Health Organization grade | Global tumor grading according to the WHO Classification of Tumours, fifth edition |
| 3. Nuclear area percent (AI model) | Ratio between total tumor nuclear area/total tumor area, by AI-based automated recognition |
| 4. Hepar-low/GPC-3-positive phenotype (AI model) | HepPar 1 expression in <50% of tumor and any degree of glypican-3 expression by AI-based automated recognition |
| 5. r-RPA (AI model) | RPA (ratio of reticulin area/total tumor area) by AI-based automated recognition |

Features 3 to 5 are based on automated recognition and quantitative analysis by our HCC AI model.
AI, artificial intelligence; HCC, hepatocellular carcinoma; RPA, reticulin proportionate area.

Figure 12. Pathologic variables identified as most significant for prognostic assessment of various HCC-related clinical outcomes across our statistical models. (Patil et al., 2025)

Conclusion

Proof-of-concept

Demonstrated that digital pathology with deep learning can objectively quantify HCC differentiation features to aid prognosis.

Independent prognostic value:

Several AI-derived metrics (nuclear area, reticulin loss, HepPar-1/GPC3 status) independently predicted HCC outcomes.

Implications

This approach could complement traditional grading, providing standardized, reproducible biomarkers.

Future work

Larger cohorts and integration into clinical workflows will be needed for validation.

References

(main article) Patil, A., Hasan, B., Park, B.U., Smith, L., Sivasubramaniam, P., Elhalaby, R., Elesawy, N., Nazif, S., DaCosta, A., Shabaan, A., Cannon, A., Lau, C., Hartley, C.P., Graham, R.R. and Moreira, R.K. (2025) 'A deep learning model of histologic tumor differentiation as a prognostic tool in hepatocellular carcinoma', *Modern Pathology*, 38, 100747. <https://doi.org/10.1016/j.modpat.2025.100747>

Takahashi, S., Sakaguchi, Y., Kouno, N., Takasawa, K., Ishizu, K., Akagi, Y., Aoyama, R., Teraya, N., Bolatkan, A., Shinkai, N., Machino, H., Kobayashi, K., Asada, K., Komatsu, M., Kaneko, S., Sugiyama, M. & Hamamoto, R. (2024) 'Comparison of Vision Transformers and Convolutional Neural Networks in Medical Image Analysis: A Systematic Review', *Journal of Medical Systems*, 48, 84. <https://doi.org/10.1007/s10916-024-02105-8>

Martins-Filho, S.N., Paiva, C., Azevedo, R.S. and Alves, V.A.F. (2017) 'Histological grading of hepatocellular carcinoma – a systematic review of literature', *Frontiers in Medicine*, 4, Article 193. <https://doi.org/10.3389/fmed.2017.00193>

ScyTek Laboratories (n.d.) Reticulum II Staining Kit – Instruction Manual. Logan, Utah: ScyTek Laboratories. Available at: <https://www.scytek.com>

Mod Pathol 38 (2025) 100747

MODERN PATHOLOGY

 **USCAP** UNITED STATES AND CANADIAN ACADEMY OF PATHOLOGY
Advancing Pathology Together

Journal homepage: <https://modernpathology.org/>

Research Article

A Deep Learning Model of Histologic Tumor Differentiation as a Prognostic Tool in Hepatocellular Carcinoma

Ameya Patil^a, Bashar Hasan^b, Byoung Uk Park^c, Lindsey Smith^d, Priya Sivasubramaniam^e, Rofyda Elhalaby^f, Nada Elessawy^f, Saadiya Nazli^f, Adilson DaCosta^f, Abdelrahman Shabaan^f, Andrew Cannon^f, Chun Lau^g, Christopher P. Hartley^f, Rondell P. Graham^f, Roger K. Moreira^{f,*}

^a Department of Laboratory Medicine and Pathology, Mayo Clinic, Scottsdale, Arizona; ^b Department of Evidence-Based Practice Center, Mayo Clinic, Rochester, Minnesota; ^c Department of Laboratory Medicine and Pathology, University of Minnesota, Minneapolis, Minnesota; ^d MySME LLC, Birmingham, Alabama; ^e Department of Pathology and Laboratory Medicine, Medical College of Wisconsin, Milwaukee, Wisconsin; ^f Department of Laboratory Medicine and Pathology, Mayo Clinic, Rochester, Minnesota; ^g Department of Computer Sciences, Rutgers University, Piscataway, New Jersey



THANK YOU!